CHEMISTRY & SUSTAINABILITY
CHEMSUSCHEM
ENERGY & MATERIALS

Accepted Article

Title: A Strategy for Simultaneous Synthesis of Methallyl Alcohol and Diethyl Acetal with Sn-β

Authors: Wenda Hu, Yan Wan, Lili Zhu, Xiaojie Cheng, Shaolong Wan, Jingdong Lin, and Yong Wang

To be cited as: *ChemSusChem* 10.1002/cssc.201701435

Link to VoR: http://dx.doi.org/10.1002/cssc.201701435

A Journal of
ChemPubSoc Europe

WILEY-VCH www.chemsuschem.org

A Strategy for Simultaneous Synthesis of Methallyl Alcohol and Diethyl Acetal with Sn-β

Wenda Hu,[a] Yan Wan,[a] Lili Zhu,[a] Xiaojie Cheng,[a] Shaolong Wan*[a, b, c] Jingdong Lin,[a, b] and Yong Wang [a, b, c, d]

Abstract: Herein we report a strategy to simultaneously produce two important chemicals namely methallyl alcohol (Mol) and diethyl acetal (Dal) from methacrolein (Mal) in ethanol solvent at low temperature with the use of Beta zeolites modified by tin (Sn-β catalysts). All Sn-β catalysts were prepared by the solid-state ion-exchange (SSIE) method, wherein the calcination step was conducted in different gas atmospheres. The one pre-calcined in Ar (Sn-β-Ar) diminishes the number of extra-framework Sn species and instead enables more Sn species exchanged into the framework as isolated tetrahedral Sn (IV), thus enhancing the catalytic activity of Meerwein-Ponndorf-Verley (MPV) reaction. The sodium-exchanged Sn-β-Ar, with the weak Brønsted acid site further diminished, leads to an even better result to Mol, thanks to the restriction of those side reactions such as acetalization, addition and etherification. Under optimized catalyst and reaction condition, the yield of Mol and Dal could reach about 90% and 96%, respectively. The possible reaction pathway, along with the complex network of side products, was proposed after a detailed investigation through the use of different substrates as the reactants. The findings of Sn-β fine-tuned through different treatment in this work, are of great significance toward understanding and manipulating the complex reaction between α, β-unsaturated aldehydes and primary alcohols.

Introduction

Methallyl alcohol (Mol) is an important chemical, widely used as a raw material in making various polymers, pharmaceuticals, pesticides and other allyllic compounds. Mol can be the precursor of 2-methyl-1,4-butanediol, which plays important parts in the pharmaceutical industry and in polyester chemistry.[1] Also, 2-methylglycidol, the epoxidation product of Mol, functions as feedstock for synthesis of biologically active compounds, cosmetics, and immunomodulators for therapy of diseases.[2a, 2b] The conventional method to prepare Mol is hydrolysis of methylallyl chloride, which would have to employ alkali, organic solvent, as well as high temperature and pressure. To avoid the use of such harsh environment, a few efforts of novel replacement have been found in the literature. A synthesis strategy of Mol through hydrogenation of methacrolein (Mal) was reported in a Japanese patent JP2000290546, where homogeneous Ru-based catalysts were applied. Alternatively, Shimasaki et al. proposed vapor phase hydrogen transfer between Mal and ethanol, catalyzed by a less expensive and heterogeneous catalyst, i.e. modified MgO.[3a, 3b] However, the process suffered a low conversion of Mal even under high temperature, and the catalyst stability is also an issue as well, especially with moisture existence. Therefore, the development of an effective but environmentally benign tactic for Mol synthesis is still needed.

The direct hydrogenation of α, β-unsaturated aldehydes like methacrolein (Mal), readily obtained by selective oxidation of isobutene,[4] requires selective activation of the carbonyl bond while retaining the active C-C double bond intact. This is difficult to achieve with the more typical approaches based on the use of noble metal catalysts. Alternatively, the Meerwein-Ponndorf-Verley (MPV) reduction, namely the hydrogen transfer reaction between alcohol and aldehyde, has long functioned as a tool for selectively reducing α, β-unsaturated aldehydes to α, β-unsaturated alcohols (like Mol), while not reducing the double carbon bond.[5a, 5b, 5c] Homogeneous MPV catalysts, such as aluminum alkoxides, are traditionally used to convert aldehyde.[1] Replacement by heterogeneous catalysts is therefore of interest. A variety of solid MPV catalysts have been reported, and successfully applied: metal oxides,[7] grafted metal alkoxides,[8] and zeolites.[9a, 9b] Among them, Sn-β has shown very good activity and selectivity for MPV reductions, acting as a strong and water-tolerant Lewis acid catalyst.[9a, 10a, 10b] The well-known examples include isomerization of glucose to fructose,[11] selective synthesis of lactic acid derivatives,[12] and chemoselectively catalyze Baeyer-Villiger oxidation of ketones to lactones,[13] etc.. Therefore, Sn-β is also expected as a promising catalyst for selectively synthesis of α, β-unsaturated alcohols (Mol) through MPV reaction in this work.

Besides the catalyst, the choice of alcohols is also a key consideration for practical application. Secondary alcohols such as 2-propanol are more often chosen as hydrogen donors and solvents for MPV reactions,[7, 9a, 10a] due to their evidently lower reduction potential and less complexity of the product distribution compared with that of primary alcohols.[14] However, primary alcohols, especially ethanol, have a lot of advantages in practical application. First, it is industrially available in large scales by a well-developed process. Moreover, the MPV product from ethanol leads to acetaldehyde, which is of higher market value than the alcohols. The direct oxidation of ethanol to aldehyde is very challenging to control, since it tends to be fully oxidized to acetic acid. With ethanol as the solvent, acetaldehyde will be further reacted and exist in its acetal form, namely diethyl acetal (Dal), which can be readily converted back to the aldehyde. An alternative is just keeping Dal as the desired product. Dal is also an important chemical, widely used as oxygenated additive for diesel fuel to reduce the

[a] W. Hu, Y. Wan, L. Zhu, X. Cheng, S. Wan, J. Lin, and Y. Wang
College of Chemistry and Chemical Engineering
Xiamen University
Xiamen 361005, China
E-mail: swan@xmu.edu.cn; Wang42@xmu.edu.cn.
[b] S. Wan, J. Lin, and Y. Wang
Collaborative Innovation Center of Chemistry for Energy Materials
Xiamen 361005, China
[c] S. Wan, and Y. Wang
National Engineering Laboratory for Green Chemical Productions of Alcohols-Ethers-Esters
Xiamen 361005, China
[c] Y. Wang
Voiland School of Chemical Engineering and Bioengineering
Washington State University
Pullman, WA 99164 , United States.

Supporting information for this article is given via a link at the end of the document.

emission of particles and NO_X, and the precursor to prepare some pharmaceuticals and perfumes.[15] Dal production is generally realized by reaction of acetaldehyde and ethanol in acid solution, or through the use of ion-exchange resins and zeolites.[16a, 16b] However, the direct use of acetaldehyde suffers from its low boiling point (294 K), toxicity and instability. Liu et al. then developed a more complicated two-step process for the synthesis, including initial oxidation of ethanol and subsequent acetalization of formed acetaldehyde with bifunctional catalysts.[17] The yield reached 70.5% after removal of water with the aid of 3A zeolites, the highest so far reported in the open literature. Relevant to this, the current approach shows advantages. As shown in Scheme 1, this route is expected not only to readily produce more valuable products, namely Mol and Dal (or acetaldehyde), but more importantly with high product yield and process efficiency.

The Sn-β catalyst is tedious and time-consuming to prepare using conventional hydrothermal synthesis routes.[9a] The post-synthesis of Sn-β has been described as an efficient replacement, using a variety of ways to introduce Sn species into the zeolite framework. Li et al. reported a solid-gas reaction of dealuminated beta zeolite with $SnCl_4$ vapor at elevated temperatures to obtain the Sn-β catalyst with a varied loadings of Sn.[18] Dijkmans's group successfully prepared 1.6 wt% Sn-β via grafting with $SnCl_4{\cdot}5H_2O$ in dry isopropanol under reflux condition.[19a, 19b] The solid-state ion-exchange (SSIE) method, as proposed by Hermans et al., has attracted a lot of attention due to its many advantages. For example, H-β zeolite can be directly used as the starting material. The long synthesis times required in the traditional method are no longer needed, and the small crystallite sizes can be maintained as well, which could be critical for reducing diffusional resistances during the reaction.[20a, 20b] The method also shows flexibility in tuning the number and the environment of Lewis acid sties as well as the amount of medium/weak Brønsted acid counterpart of the catalyst by simply changing the pre-treating conditions. Recently, Hermans and Hammond et al. reported a modified post synthesis SSIE method,[21a, 21b] which was pre-heated in inert gas instead of flowing air. The modified method was claimed to help diminish extra-framework Sn species and generate more isolated tetrahedral Sn(IV), leading to increased Lewis acid at the cost of diminished moderate/weak Brønsted acid sites.

It is known that there are also weak Brønsted sites (net silanol groups) and some extra-framework Sn species besides the framework isolated tetrahedral Sn(IV) sites, especially in the post-syntheis Sn-β zeolite.[18] Each of these active sites could catalyze different reactions independently or in a concerted way, especially in the cases where many or all possible reactions may occur. The coexistence of various Brønsted and Lewis acid sites could lead to a variety of reactions and a complex network. Therefore it appears to be critical to control the relative amounts of the different acid sites, the determining factor for selectivity of the desired products. Indeed, recent reports show that the catalysts can not only catalyze the MPV reaction, but also play an important role in several other reactions. Roman-Leshkov et al. hypothesized that the acid–base characteristics of the hydroxyl groups of the Sn-β are associated with the etherification steps, as well as the acetalization side reaction.[22] The acetalization is actually quite common in alcohol solvent on Sn-β catalyst, as observed by Sels et al.[19a] Later Roman-Leshkov et al.[23] also reported that Sn-β can catalyze the carbon carbon coupling between carbohydrates and formaldehyde. It is still not very clear about the exact mechanism or specific active site of the catalyst. Along with this line, the evaluation of the reaction network involved in our work could shed further light on the insight of the reaction mechanism over Sn-β catalysts.

Herein, we first report a facile strategy to simultaneously synthesize Mol and Dal (or acetaldehyde) in a high yield at low temperature with SSIE post-synthesized Sn-β. The reaction conditions were optimized, and a complex reaction pathway will be revealed in detail. Furthermore, we systematically investigated a series of catalysts prepared by different pre-treatment measures, the structure and acid property of which were all thoroughly characterized. The correlation of catalyst properties with reaction selectivity and activity is especially emphasized.

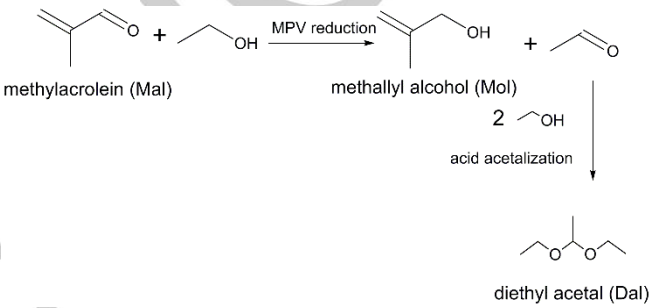

Scheme 1. MPV reduction and tandem acid acetalization of acetaldehyde.

Results

Catalyst characterization

The topology of beta zeolite was retained intact for the prepared deAl-β, Sn-β Sn-β-Ar and Sn-β-Ar-Na, as confirmed from the XRD results in Figure 1. This indicates no destruction of zeolite framework occurred through the acid treatment, incorporation of Sn and calcination in air or argon, consistent with earlier reports.[20a, 20b, 21a] A small amount of SnO_2 does exist in Sn-β, evidenced by occurrence of the reflection peaks at 26.6°, 33.9°, and 51.8°, ascribed to the (110), (101) and (211) planes of rutile-like SnO_2.[24] However, very weak peaks were found in those three reflections for Sn-β-Ar and Sn-β-Ar-Na, suggesting little existence of such extra-framework SnO_2.

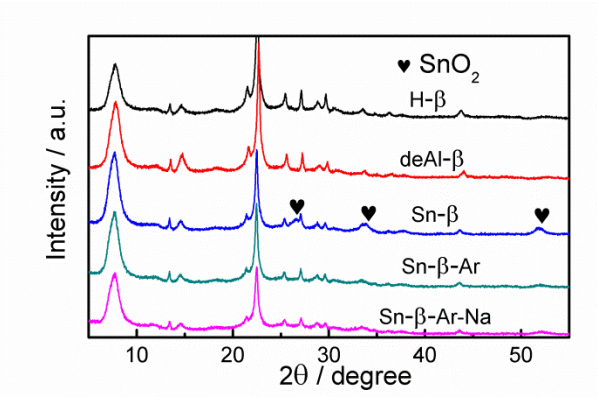

Figure 1. Powder XRD patterns of different Beta zeolites.

The physicochemical properties of the catalysts evaluated in this work are summarized in Table 1. Both the dealuminated and Sn-grafted zeolites exhibit BET surface areas and micropore volumes similar to parent H-Beta, again suggesting no significant structure damage during the treatment, and in line with the previous XRD results. The slightly increased specific surface area of deAl-β is probably due to the removal of framework Al and consequent appearance of silanol nests.[18] The molar ratio of Si/Al increased from 12.5 of initial zeolite to 833 after dealumination, indicating that most Al was removed from the zeolite structure. The molar ratios of Si/Sn are identical for Sn-β and Sn-β-Ar, and the extra-framework SnO_2/deAl-β also has a close range of Si/Sn ratio to ensure a comparable Sn content. The SEM pictures in Figure S1 show that the average crystallite sizes of both Sn-β and Sn-β-Ar (60- 80 nm) are much smaller than the reported conventional synthesized Sn-β, with approximately 1000 nm crystallite diameter.[18, 25]

Table 1. Physicochemical properties of catalysts.

Entry	Catalyst	Treatment	S_{BET}[a] [m^2g^{-1}]	V_{micro}[b] [cm^3g^{-1}]	Molar ratio[c]
1	H-β	-	460	0.20	Si/Al 12.5
2	deAl-β	H^+	498	0.21	Si/Al~833
3	Sn-β	H^+&SSIE	467	0.18	Si/Sn~18
4	Sn-β-Ar	H^+&SSIE& Ar	437	0.17	Si/Sn~18
5	Sn-β-Ar-Na	H^+&SSIE& Ar&Na	489	0.17	Si/Sn~18 Si/Na~69
6	SnO_2/de Al-β	H+&mixing	410	0.17	Si/Sn~11

[a] Specific surface areas obtained by BET method. [b] Calculated from t-plot. [c] Determined by EDS.

The FT-IR spectra of H-β, deAl-β, Sn-β, and Sn-β-Ar are shown in Figure 2. The parent H-β zeolite demonstrates nearly no absorption at 950 cm^{-1}, which is typically assigned to Si–O stretching vibrations of Si–OH groups occurring at structure defects.[26a, 26b] The peak intensity is remarkably enhanced for deAl-β, attributed from the formation of silanol nests at the vacant sites after acid treatment. The near disappearance again of this peak in Sn-β and Sn-β-Ar suggested that the introduction of Sn has been successfully incorporated into the dealuminated framework, forming the tetrahedral Sn and thus turning off the nests of silanol due to the incorporation of Sn into those defect framework sites. In addition, the Sn-β and Sn-β-Ar present increased absorbance intensity at approximate 575 cm^{-1}, probably owing to the enhanced framework vibration through the Sn incorporation.[26a, 27]

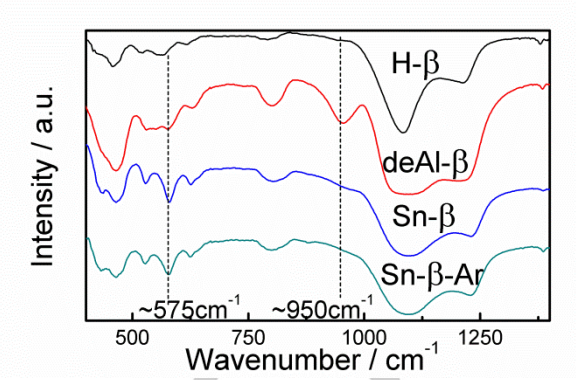

Figure 2. FT-IR spectra of H-β, deAl-β, Sn-β and Sn-β-Ar.

The coordination state of Sn can be identified by diffuse reflectance ultraviolet visible (UV-vis) spectra, as seen in Figure 3. The deAl-β, recorded as the bottom line, features fairly low absorption, suggesting little electronic transition occurring. The Sn-β detects a peak centered at 202 nm, as well as a shoulder at higher wavelength. The former is assigned to the ligand-to-metal charge transfer from O^{2-} to Sn^{4+}, which is characteristic of isolated tetrahedrally coordinated Sn in the framework of deAl-β; while the latter is typically caused by the formation of extra-framework SnO_2 species.[20b, 28a, 28b, 28c] However, the Sn-β-Ar shows a much more intense peak at 202 nm, but merely no absorption at higher wavelength. This indicates that framework Sn species are dominant in Ar-preheated Sn-β, with much less extra-framework SnO_2 compared with air-treated counterpart, consistent with the XRD results aforementioned. On the contrary, pure SnO_2 presents significantly broad absorption from the about 200 nm to 300 nm, centering at 250 nm,[29] since the coordination state is totally different from the framework Sn of beta zeolite. And the framework Sn is also detected by Raman spectroscopy, as displayed in Figure S2.

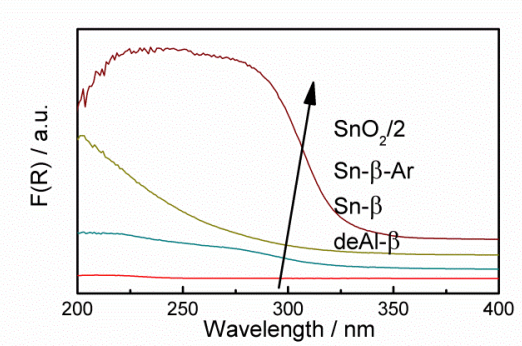

Figure 3. UV-Vis spectra of deAl-β, Sn-β, Sn-β-Ar and SnO_2.

The acid properties of catalysts were characterized by FT-IR with pyridine adsorption (Figure 4). The H-β possesses both Brønsted and Lewis acid sites, characterized by the band at 1540 cm^{-1} and 1450 cm^{-1} respectively.[18, 28c, 30a, 30b] The near disappearance of those bands in the dealuminated zeolite suggests that most of both acid sites were removed after acid treatment. The peaks at 1446 cm^{-1} and 1594 cm^{-1}, vibrations of stretching modes of hydrogen-bonded pyridine corresponding to hydroxyl groups of zeolites,[31a, 31b, 31c] are significantly enhanced probably due

to the formation of silanol nests. The subsequent incorporation of Sn greatly enhances the Lewis acidity in Sn-β, Sn-β-Ar and Sn-β-Ar-Na, as confirmed by the strong adsorption at 1611, 1490 and 1450 cm^{-1}. Those are typical vibration modes of the pyridine-rings adsorbed on the isolated tetrahedral Sn (IV) species in the beta zeolite.[31c, 32] The vibrations of hydrogen-bonded pyridine are decreased a bit, when comparing Sn-β with Sn-β-Ar, indicating that more silanol nests are occupied. The type of peak of Sn-β-Ar-Na is identical to Sn-β-Ar, but the peaks corresponding to hydroxyl groups at 1446 and 1594 cm^{-1} are lowered significantly due to the presence of sodium ions. This phenomenon indicates that the protons of the silanols are successfully replaced with sodium, thus resulting in a weakened Brønsted acidity, as will be discussed in the catalytic activity section. Combining NH_3-TPD and FT-IR with pyridine adsorption, the acid concentrations were provided in Table S4.

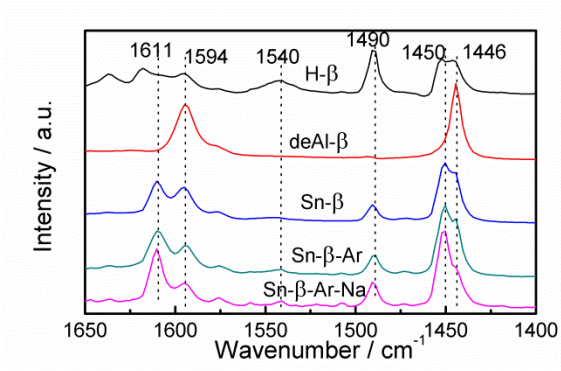

Figure 4. FT-IR spectra of H-β, deAl-β, Sn-β, Sn-β-Ar and Sn-β-Ar-Na with pyridine adsorption at 373 K and evacuation at 423 K.

Catalytic activities of Sn-β

Sn-β catalyst was studied over a wide range of reaction conditions (such as temperature, substrate concentration, types of alcohols used for MPV, and catalyst loading) to optimized the yield of Mol. As shown in Figure 5, under the optimized conditions over Sn-β, Mol is the primary product from Mal, derived from MPV reduction with ethanol. Dal from the acetalization of the aldehyde with ethanol is another major product. The yields of Mol and Dal reach about 71% and 94% respectively in 2 h, and then slightly decrease due to secondary reactions. No acetaldehyde was detected, which should be primarily produced from ethanol through the MPV reaction, prior to the conversion to its acetal form. This appears to suggest that the MPV reaction is the rate-limiting step in Dal production, while the subsequent acetalization step is not kinetically relevant.

The major byproducts are C_{8+} and C_6 species, mainly resulting from the acetalization and addition-derived product of Mal respectively. The former one shows a typical feature of intermediate product, with the yield first reaching the highest in 1 h and then continuously dropping to nearly disappearance. This suggests that there is an equilibrium between acetal product and Mal. As Mal is continuously converted to Mol, Mal is depleted but replenished via the decomposition of acetal product. However, the yield of C_6 addition products follow the characteristic curve of stable primary products, which increase monotonously and then reach nearly stable to 20% as the increase of Mal conversion. There are also some minor products detected, including the C_6 etherification product and isobutanol (Ibol) probably derived from Mol. More details about these byproducts will be discussed in discussion section Reaction conditions such as temperature, substrate concentration, and catalyst loading also affect the selectivities and the yields to Mol, Dal, and other side products (Figure S3-4 and Table S1-3).

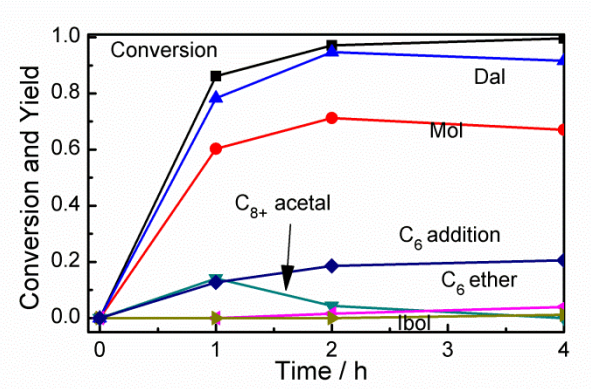

Figure 5. Catalytic activity of Sn-β with time-on-stream. Optimized reaction conditions: reflux, 350 K, 0.9 mmol Mal, 80 mmol ethanol and 0.5 g Sn-β.

Catalytic activities with Sn-β-Ar

Compared to the results above, Sn-β-Ar catalyst exhibits a superior catalytic activity toward the desired products under the same optimized reaction conditions, as illustrated in Figure 6. The yields of Mol and Dal rapidly rise to 81% and 93% respectively at 1 h on time stream, and the C_{8+} acetalization product is now cut into 4.5% from 14% in Figure 5 of Sn-β. With the subsequent consumption of the C_{8+} side product, the released Mal will be further reacted to form Mol, which then reaches up to 85% yield in 2 h. The C_6 addition product is also decreased to 15%, compared to 20% in Sn-β. The overall mass balance based on Mal is well closed over the entire time-on-stream examined, which mainly consists of MPV product Mol, C_{8+} acetal and C_6 addition product before 2 h.

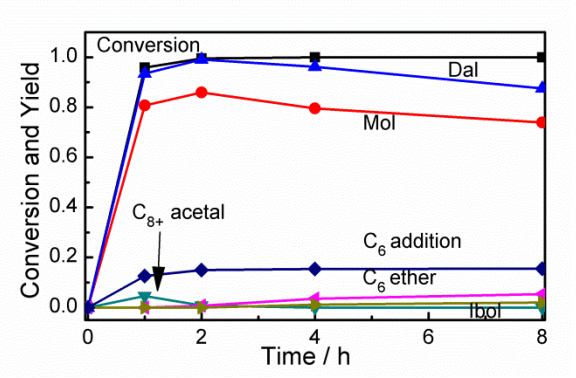

Figure 6. Catalytic activity of Sn-β-Ar with time-on-stream. Optimized reaction conditions: reflux, 350 K, 0.9 mmol Mal, 80 mmol ethanol and 0.5 g Sn-β-Ar.

The drop in Dal yield is quite striking after 2 h. To shed light on the mechanism of this phenomenon, the test was intentionally extended to a long period of 8 h to exaggerate the effect. As shown in Figure 6, the yield of Dal is further declined to 87% after 8 h. The significant disappearance of Dal is probably due to the evaporation of acetaldehyde, due to its low boiling point about 294 K. Since it is much below the reflux temperature 350 K, the condenser used in the work is probably not capable to completely condense acetaldehyde vapor back into the flask. Therefore, Dal would remain relatively stable in less than 4 h, staying under equilibrium with acetaldehyde (though under detected level). However, if holding on the reaction long enough, the slow but continual evaporation and loss of acetaldehyde would shift the equilibrium and eventually consume all the Dal, as seen in Figure S3b. With the prolonged reaction time, two minor secondary products, i.e. the C_6 etherification product and Ibol also gradually build up, which appears to be consistent with the slight decrease in Mol yield.

Catalytic activities with Sn-β-Ar-Na

The Na-exchanged Sn-β-Ar zeolite further improved the performance over the un-exchanged counterpart, which was also applied in improving the selectivity of lactic acid produced by sugar.[33] As exhibited in Figure 7a, the yield of Mol and Dal products now reach 90% and 96%, respectively, in 3 h. The level of intermediate C_{8+} acetal remains at a low level in 1 h, followed by nearly complete disappearance after 2 h time-on-stream. The striking effect is the depression of the side reactions over the Na-exchanged zeolite. The C_6 addition product is notably reduced to 10% over the 4 hours' reaction, and there is barely C_6 ether product and Ibol detected. The enhancement of the desired Mol product and the inhibition of C_6 addition byproduct can be clearly seen in the direct comparisons over the three Sn-β catalysts, as exhibited in Figure 7b.

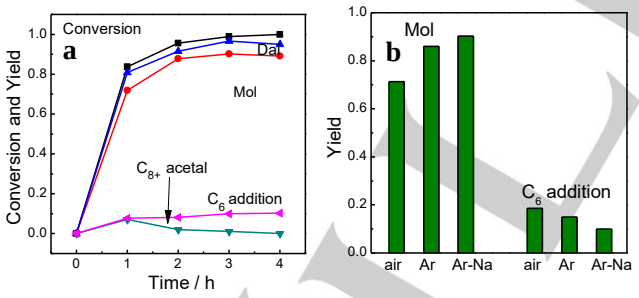

Figure 7. Catalytic activity with Sn-β-Ar-Na (a) and comparison of best catalytic results with three Sn-β catalysts (b) air: Sn-β, Ar: Sn-β-Ar, Ar-Na: Sn-β-Ar-Na. reaction conditions: reflux, 350 K, 0.9 mmol Mal, 80 mmol ethanol and 0.5 g Sn-β-Ar-Na.

The stability of Sn-β-Ar-Na zeolite was studied. There is a gradual deactivation during the four consecutive recycle runs (Figure S5). However, catalysts can be readily regenerated by calcination in air for 5 hours at 773 K (Figure S5). The encouraging results suggest a great potential for this catalyst in the practical application toward the simultaneous production of Mol and Dal.

Discussion

Results from different catalysts

A variety of catalysts have been tested under the optimized conditions described above in order to fully understand the reaction network and the relationship and role of specific acid sites. As shown in entry 1 of Table 3, there was no activity in the blank run, where only reactants but no catalysts were loaded. H-β catalyst can achieve nearly 30% conversion, resulting in mostly the C_{8+} acetalization product of Mal, but no MPV products were detected. The dealuminated counterpart, deAl-β shows a diminished activity, leading to about 24% conversions and the same C_{8+} acetal species as dominant products. It is generally believed that the Brønsted acid sites can effectively catalyze the acetalization reaction.[34] As evidenced in Figure 4, there are both Brønsted and Lewis acid sites in H-β. The former are mainly ascribed to the framework Al (generating strong Brønsted acidity), while the latter more related with partially coordinated Al atoms and extra-framework Al.[35] This clearly suggests that the relative strong Brønsted sites in H-β can effectively catalyze the acetalization of Mal with ethanol, while the Lewis acid sites present in H-β lack the ability to activate the MPV reaction. The removal of the framework Al in deAl-β eliminates those strong Brønsted acid sites, but moderate or weak Brønsted acidity ascribed to the surface or the nest hydroxyl groups are still present, as shown in FTIR spectra of Figure 2 and Figure 4. These acid sites are active enough to produce an acetalization product of Mal, but to a less extent.

The subsequent introduction of Sn into the framework forms strong Lewis acid sites,[9a, 36] accompanied with the decrease of nest hydroxyl groups (moderate or weak Brønsted acid sites). As a result, Mol and Dal are shown as the major products, while the selectivity toward acetalization of Mal was suppressed to a low level instead. The reason why Dal yield, also derived from acetalization, was not depressed will be discussed later. Another side product from addition to the double C-C bond also occurs to a notable level. We suggest that tetrahedral Sn Lewis acid sites in Sn-β framework are responsible for the MPV reaction, rather than the extra-framework SnO_2.[23, 37] To further prove this argument, extra-framework SnO_2/deAl-β was synthesized and employed under the same reaction condition. As seen in entry 5, the conversion is comparable to that of deAl-β, resulting in no Mol but only acetalization products. When 'pure' SnO_2 served as catalyst, there was no reaction. This demonstrates that extra-framework Sn is not catalytically active in the MPV, or the addition reaction.[21a] Enhanced performance is achieved with the employment of Sn-β-Ar, as shown in entry 8 of Table 3 and Figure 7b. The superior performance may be the result of the pre-heating step wherein the Ar might increase the dispersion between Sn precursor and the dealuminated zeolite, so that more Sn react with the silanol nests and embed into the framework, resulting in a greater Lewis acidity (as demonstrated in Figure 3). Accordingly, the nest hydroxyl groups are diminished, lowering weak/moderate Brønsted acidity as shown in Figure 4. The Na-exchanged Sn-zeolite could further diminish the remained Brønsted acidity. The active sites in the Sn-β catalyst are those hydrolyzed active Sn framework, where the hydroxyl groups on or near the active Sn sites could lead to somewhat Brønsted acidity.[22] With the sodium ion-exchange step, those protons near the Sn sites could be readily replaced.[38] Besides, the Na-exchanged deAl-β also shows

a reduced activity as illustrated in Entry 4 of Table 3, which is due to the fact that the unoccupied nest or surface hydroxyl groups could also be exchanged, resulting in weakened Brønsted acidity. Overall, the high conversion and selectivity over MPV through Lewis acid sites is favored over the acetalization and addition reactions on Brønsted acid sites, as referred in Entry 9 and Figure 7b. It should be noted that the calculated TON numbers referring to the MPV products (i.e. Mol) produced on each Lewis acid site are comparable over the 3 Sn-β catalysts as shown in Table S4, where the numbers of Lewis and Brønsted acid sites are estimated using the results from ammonia TPD and pyridine-IR. These results suggest that the superior performance from Sn-β-Ar-Na compared to that of Sn-β-Ar and Sn-β is due to the increased number of Lewis acid sites, which enhances MPV products, and the diminished Brønsted acid sites, which limits the side reactions. The mechanism over the complex reaction network will be next discussed in detail.

Table 3. Catalytic activity of Sn-β and other catalysts.[a]

Entry	Catalyst	Conv. [%]	Selec. [%] Mol	Yield [%] Mol	Dal	C_{8+}acetalization	C_6addition
1	Blank	-	-	-	-	-	-
2	H-β	29.6	-	-	-	26.0	-
3	deAl-β	24.0	-	-	-	21.0	-
4	deAl-β-Na	8.7	-	-	-	6.2	-
5	SnO_2/deAl-β	22.9	-	-	-	20.5	-
6	SnO_2	-	-	-	-	-	-
7	Sn-β[b]	97.2	73.4	71.3	94.7	4.4	19.6
8	Sn-β-Ar[b]	99.5	85.4	85.0	99.1	0.8	14.0
9	Sn-β-Ar-Na[b]	98.9	91.2	90.2	96.6	0.1	9.9

[a] Reaction conditions: reflux, 350 K, 1 h, 1.8 mmol of Mal, 80 mmol of ethanol and 0.2 g catalyst. [b] At optimal condition.

Insights into the reaction pathway

Based on the extensive experiments and analysis above, the proposed reaction network is displayed in Scheme 2. It is clear that isolated Sn Lewis sites determine MPV productivity and the Brønsted acid sites can effectively catalyze the acetalization reaction. The intriguing part is the third primary product of C_6 addition derived from Mal and ethanol, which took a significant effort to identify. As shown in the Scheme, the possible pathway is that the C=C double bond of Mal is first attacked by ethanol to form C_6 intermediate via 1, 4-addition, staying in equilibrium with its aldehyde isomer, which is common in reactions catalyzed by homogeneous Sn catalysts.[39] The latter isomer then conducts a MPV reaction with ethanol to obtain the alcohol counterpart and acetaldehyde. The formed aldehyde will subsequently convert to Dal, which may explain its higher yield than Mol during the whole reaction time course. This is further supported by the fact that Dal roughly equals to the sum of Mol and C_6 addition. C_6 ether and Ibol were seen as the two minor products derived from Mol. The formation of the C_6 ether is quite straightforward, as it can be derived from Mol and ethanol. Ibol generation is more complex; it can be acquired either directly through reducing C=C bond of Mol with ethanol hydrogen fragments,[40] or via the two-step route, i.e. the first isomerization of Mol to isobutyraldehyde and subsequent MPV reaction with ethanol.[41a, 41b]

It should be noted that the yield of C_6 addition product decreased from 20 to 15% after the replacement of Sn-β with Sn-β-Ar, and further declined to 10% with Sn-β-Ar-Na. Dusselier et al. reported that a vinyl group in conjugation with a carbonyl could easily undergo a 1, 4-nucleophilic addition with alcohol under homogeneous metal catalysts like Sn chloride salts, resulting in the apparent anti-Markovnikov addition to the olefin. Their further experiments also show that the reaction could be assisted by Brønsted acidity, as evidenced by the sole use of H_2SO_4.[39] Our results here appear to suggest that the reaction is catalyzed mainly by Lewis acid sites, but possibly enhanced somewhat by the coexistence of weak or moderate Brønsted acid site. As illustrated in Scheme 2, the production of C_6 addition alcohol involves several sequential steps such as the 1,4-nucleophilic addition, isomerization and MPV reaction. No such C_6 product occurs under the case of H-β or deAl-β in entry 2 and 3 of Table 3, since the last MPV step can't proceed due to the lack of strong Lewis acidity derived from framework Sn. However, the former two steps could be facilitated by moderate or weak Brønsted acid sites. This is consistent with the overall yield following the order of Sn-β > Sn-β-Ar > Sn-β-Ar-Na, as consistent with the diminished Brønsted acidity.

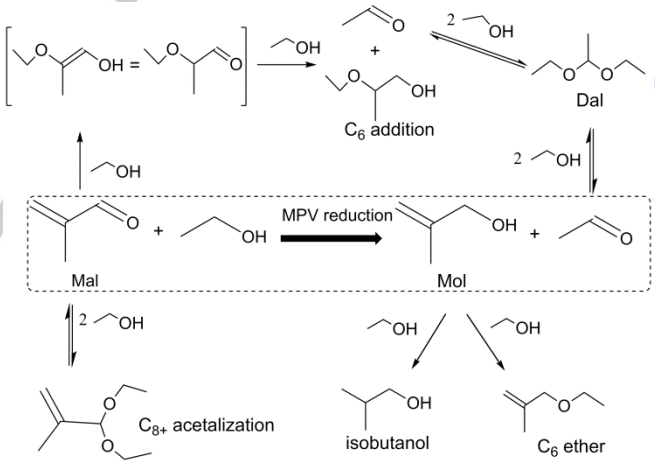

Scheme 2. Proposed reaction network involved with the reaction of Mal in ethanol solvent on Sn-β.

Another issue unsolved yet is the effects of Brønsted and Lewis acid sites on the formation of the acetal products. As discussed before, the C_{8+} acetalization product of Mal appears to be suppressed on catalysts with the reduced Brønsted acid sites such as catalysts by Ar pre-treatment and Na-exchange (in Figure 6 and 7 respectively), compared to that from the Sn-β (in Figure 5) under 1 h reaction. However, this may be more related with the equilibrium between Mal and the acetal products, as more Mal converted to Mol in the former two cases will result in less C_{8+} acetalization product under equilibrium. Indeed, a high yield of Dal (>95%) is achieved in all of those three catalysts, regardless of their distinctive Brønsted acid

properties, indicating that other factor like the Lewis acid sites should also play an important role in the acetalization. Acetalization by both Lewis and Brønsted acid has been previously reported,[34, 42] but the role of different acid sites in the complex catalyst like Sn-β hasn't been fully clarified yet according to the best of our knowledge. To further provide insight into the effect of Brønsted/Lewis acidity on the acetalization, a simple reaction just using acetaldehyde and ethanol as the substrates was performed under various catalysts. Without the complex reactions involved like those in Scheme 2, the results are quite straightforward and well distinguished corresponding to the varied acid properties, as shown in Figure 8. On dealuminated zeolite deAl-β, which has only weak or medium Brønsted acid sties from its rich of terminal or defect silanols, 30% yield of Dal was reached. On Na-exchanged deAl-β-Na (Na exchange once) and deAl-β-Na3 catalysts (Na exchange 3 times), Dal yields are significantly reduced to 1.5% and 0.8%, respectively, due to the nearly complete removal of those weak Brønsted acid sites by Na-exchange process. In addition, it was also found that Dal yield reduced from 33% to 23%, when the working catalyst was switched from Sn-β-Ar to Sn-β-Ar-Na3 catalysts. These results clearly confirm the catalytic role of Brønsted acidity on Dal formation. On the other hand, Sn-β-Ar-Na3 catalysts exhibit a high yield of Dal up to 23%, compared to that of 0.8% from deAl-β-Na3. There will barely exist any weak Brønsted acid sites in Sn-β-Ar-Na3, as that in deAl-β-Na3 after three times Na ion exchange. The strong Lewis acidity due to Sn incorporation in the former catalyst is thus the only reason responsible for the consequent higher activity toward the acetalization. Based on these results, it clearly demonstrates that the acetalization reaction is not solely catalyzed by Brønsted acid sites, but also contributed from the Lewis acid sites, which actually play a dominant role in Sn-β-Ar and its ion exchanged counterpart. Along with this line, similar experiments have been conducted to evaluate the mechanism over other minor products including C_6 ether and isobutanol. As shown in the Figure S6, it appears that the dominant factor toward the etherification is the weak/medium Brønsted acid sites remained on the Sn-β or Sn-β-Ar.

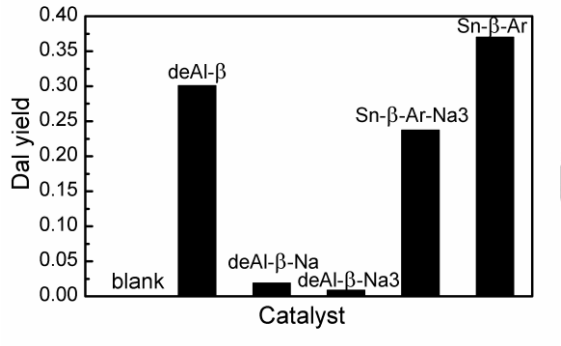

Figure 8. Acetalization of acetaldehyde with ethanol using different catalysts. Reaction conditions: 0.8 mmol acetaldehyde, 80 mmol ethanol, 350 K, 10 min, 0.1 g catalysts.

Conclusions

We have developed an approach to simultaneously synthesize chemical intermediates Mol and Dal at low temperatures, employing a SSIE post-synthetic Sn-β. Upon pre-treating the catalyst with Ar prior to calcination and sodium exchange, the yield of Mol and Dal both referenced to Mal reactant reached up to 90% and 96% respectively. Mol derived from the MPV reaction is believed to be realized by the Sn Lewis acid sites, while Dal from the acetalization of acetaldehyde could be catalyzed by both moderate or weak Brønsted and Lewis acid sites. The Sn-β-Ar was prepared by pre-heating Sn-β in Ar gas flow before air calcination (Sn-β-Ar), which diminished the number of extra-framework Sn species and instead enabled more Sn species to be exchanged into the framework as isolated tetrahedral Sn (IV). As a result, the selectivity toward Mol is enhanced, while the side reactions including acetalization and addition are restrained. The sodium-exchanged catalyst can further diminish the weak Brønsted acid, resulting in a higher yield of desired MPV products. With extended reaction time, Dal gradually converts back to form acetaldehyde, which could be evaporated out and collected in an outside condenser. Mol also slowly reacts to form Ibol and C_6 ether. The reaction network of Mal and ethanol is described over the Sn-β catalysts, and the mechanistic insight can be of great importance to understand and manipulate the complex reactions between α, β-unsaturated aldehydes and primary alcohols. Moreover, we clearly demonstrate through direct experimental results that the acid properties of post-synthetic Sn-beta zeolite can be fine-tuned via simple pretreatment like Ar-preheating and alkali ion-exchange process, thus precisely controlling the reaction selectivity toward the desired products.

Experimental Section

Chemicals and materials

Methacrolein (95%), methallyl alcohol (98%), diethyl acetal (95%), acetaldehyde (99.5%) were obtained from Aladdin Reagent Co. Ltd. (Shanghai, China). Tin (II) acetate was purchased from J&K Chemical Technology. Ethanol, isopropanol, isobutanol, sodium nitrate, commercial H-β zeolite (Si/Al=12.5), HNO_3 (65%-68%) were supplied by Sinopharm Chemical Reagent Co. Ltd. (Shanghai, China) and used without further purification.

Catalyst synthesis

The zeolites Sn-β and Sn-β-Ar were prepared following the similar methods reported by Hermans and Hammond et al.[20a, 21b] Specifically, H-β (Si/Al=12.5) was dealuminated by treatment in HNO_3 solution (65%-68% HNO_3, 373 K, 20 h, 20 mL g^{-1} zeolite). The acid-treated powder was then filtered, washed thoroughly with deionized water, and dried at 383 K overnight. The dealuminated zeolite (denoted as deAl-β) was then grafted with tin through the solid-state ion-exchange (SSIE) method, by grinding with the appropriate amount of tin (II) acetate in a pestle and mortar. The obtained mixing powder was finally calcined in tubular reactor to obtain the working catalysts, namely Sn-β and Sn-β-Ar. The former one was calcined under air flow at 823 K for 3 h, as described in Hermans' initial research.[20a] The latter, labeled as Sn-β-Ar, was heated up to 823 K (10 K min^{-1} ramp rate) first in a flow of Ar (3 h) and subsequently in air (3 h) for a total of 6 h, referenced by their latest

modified method.[21a, 21b] Sodium exchanged Sn-β-Ar (Sn-β-Ar-Na) was carried out post-synthetically. The calcined Sn-β-Ar was soaked into a 1.0 M $NaNO_3$ solution (50 mL g^{-1} zeolite) and the mixture was stirred at 353 K for 12 h. The solid sample was recovered by filtration and washed with distilled water. After being dried at 383 K overnight, the sample was calcined at 773 K for 5 h. For comparison, the deAl-β supported tin oxides (denoted as SnO_2/deAl-β) were also prepared via mechanical mixing of deAl-β with SnO_2, followed by calcination at 823 K for 12 h.[28c]

Catalyst characterization

The surface areas of the samples were measured by nitrogen physisorption on a Micromeritics ASAP 2020 M instrument. Before the adsorption, samples were degassed at 573 K for 3 h. The total surface area was calculated via the Brunauer−Emmett−Teller (BET) equation and the microporous pore volume was determined using the t-plot method.

Scanning electron microscope (SEM) was obtained by Zeiss sigma microscope, with energy dispersive X-ray spectroscopy (EDS) measurements analyzing the chemical compositions. X-ray diffraction (XRD) patterns of samples were recorded on Rigaku Ultima IV X-ray diffractometer with CuKα radiation source (40 kV and 30 mA) from 5° to 60° and a scan speed of 2θ=10.0°/min.

Fourier transform infrared (FT-IR) spectra were collected in transmission mode as KBr pellets using a Nicolet 6700 spectrometer equipped with a DTGS detector. The FT-IR instrument was also used to collect information for pyridine adsorption. Briefly, a self-supporting pellet of the sample was placed in the flow cell and evacuated under reduced pressure at 673 K for 1 h. After cooling to 373 K, the samples were saturated with pyridine vapor and then evacuated at 373 k and 423 K respectively. Spectra were recorded at the same temperature in the 4000−650 cm^{-1} range by using co-addition of 32 scans at a resolution of 4 cm^{-1}.

NH_3-temperature-programmed desorption (NH_3-TPD) was carried out. Typically, 0.2 g sample was loaded and pretreated in a quartz reactor with high-purity He (99.999%) flow at 573 K for 1 h, followed by cooling down to 373 K. The adsorption of NH_3 was performed at 373 K in an NH_3-He mixture (5 vol % NH_3) for 2 hours to ensure the saturation of the acid sites. Then, the temperature was raised to 1173 K at a rate of 10 K min^{-1}. During the desorption process, the desorbed NH_3 was absorbed by 0.01 mol L^{-1} HCl solution and quantified via a counter titration with 0.01 mol L^{-1} NaOH solution in the presence of mixed indicator (0.1% bromocresol green and 0.2% methyl red). The number of total acid sites titrated by molecular ammonia was estimated from values using the following equation: Total acid density (μmol g^{-1})= $n(NH_3)/m$= $(c_1V_1-c_2V_2)/m$, where c_1 is the concentration of HCl solution, V_1 is the volume of HCl solution; c_2 is the concentration of NaOH solution, V_2 is the volume of NaOH solution and m is the mass of catalyst. The ratio of Lewis and Brønsted acid sites were derived from the deconvoluted peak areas of pyridine FT-IR adsorption in Figure 4 (i.e. the sum of 1594 and 1446 cm^{-1} referring to medium/weak Brønsted acid site, while the total of 1611, and 1450 cm^{-1} for Lewis counterpart), followed by an empirical procedure.[19a] From the total acidity via NH_3-TPD and the ratio of Lewis to Brønsted acid sites via FTIR of pyridine adsorption, acid concentrations are calculated and summarized in Table S4.

Diffuse reflectance ultraviolet−visible (UV−vis) spectra of samples were recorded in the region of 200−400 nm on a Varian Cary 5000 UV−vis spectrophotometer in Kubelka-Munk units using $BaSO_4$ as reference. Raman measurements were carried out on Xplora Raman spectrometer with the 638 nm source.

Catalytic Evaluation

The simultaneous synthesis of Mol and Dal was performed in a 10 ml round-bottom flask immersed in an oil bath, equipped with a condenser, a thermometer, and a magnetic stirrer. Typically, 1.8 mmol of methacrolein and 80 mmol of the ethanol were introduced in the flask with 0.2-0.5 g catalysts. The mixture was subsequently heated to 350 K and allowed to react for a defined time under vigorous stirring. Small aliquots were withdrawn at different time intervals to investigate the catalytic activity of time-on-stream. A variety of reaction conditions such as different alcohols, temperature, catalyst amount, and substrate ratio were investigated to achieve an optimized yield and selectivity. The withdrawn samples after filtration were analyzed by GC-MS with a HP-5 capillary column (30 m×0.25 mm×0.25 μm), and gas chromatography (Thermo Trace 1310) with a HP-5 capillary column (60 m×0.32 mm×0.25 μm), where 1,4-dioxane served as internal standard. Note that the yields of Mol and Dal are both referenced to Mal.

The spent catalysts were recovered for subsequent stability tests, being first filtered and dried in an oven at 383 K overnight, followed by calcination in a muffle furnace for 5 hours at 773 K (5 K min^{-1} ramp rate).

Acknowledgements

This work was supported by the Major Research Plan of National Natural Science Foundation of China (No. 91545114, and No. 91545203), the National Natural Science Foundations of China (No.21576227) the National Thousand Talents Program of P.R. China, and the 985 Program of the Chemistry and Chemical Engineering disciplines of Xiamen University.

Keywords: Sn-β • Lewis acid • weak Brønsted acid• MPV • acetalization

[1] X. Liu, X. Wang, Q. Liu, G. Xu, X. Li, X. Mu, *Catal. Today* **2016**, 274, 88-93.

[2] a) A. Wróblewska, E. Ławro, E. Milchert, *Ind. Eng. Chem. Res.* **2006**, 45, 7365-7373; b) A. Wróblewska, M. Rzepkowska, E. Milchert, *Appl. Catal., A* **2005**, 294, 244-250.

[3] a) M. Ueshima, Y. Shimasaki, *Catal. Lett.* **1992**, 15, 405-411; b) Y. Shimasaki, M. Ueshima, *Catal. Today* **1993**, 16, 563-569.

[4] S. R. G. Carrazfin, C. Martfn, V. Rives , R. Vidal, *Appl. Catal., A* **1996**, 135, 95-123.
[5] a) J. F. Miñambres, A. Marinas, J. M. Marinas, F. J. Urbano, *J. Catal.* **2012**, 295, 242-253; b) Y. Zhu, G. Chuah, S. Jaenicke, *J. Catal.* **2004**, 227, 1-10; c) Y. Zhu, G. Chuah, S. Jaenicke, *J. Catal.* **2006**, 241, 25-33.
[6] G. K. Chuah, S. Jaenicke, Y. Z. Zhu, S. H. Liu, *Curr. Org. Chem.* **2006**, 10, 1639-1654.
[7] M. Chia, J. A. Dumesic, *Chem Commun* **2011**, 47, 12233-12235.
[8] Y. Zhu, S. Jaenicke, G. K. Chuah, *J. Catal.* **2003**, 218, 396-404.
[9] a) A. Corma, M. E. Domine, L. Nemeth, S. Valencia, *J. Am. Chem. Soc.* **2002**, 124, 3194-3195; b) Y. Zhu, G. Chuah, S. Jaenicke, *Chem. Commun.* **2003**, 35, 2734-2735.
[10] a) A. Corma, M. E. Domine, S. Valencia, *J. Catal.* **2003**, 215, 294-304; b) P. Ferrini, J. Dijkmans, R. De Clercq, S. Van de Vyver, M. Dusselier, P. A. Jacobs, B. F. Sels, *Coordin. Chem. Rev.* **2017**, 343, 220-255.
[11] Y. Román-Leshkov, M. Moliner, J. A. Labinger, M. E. Davis, *Angew. Chem. Int. Ed.* **2010**, 49, 8954-8957.
[12] M. S. Holm, S. Saravanamurugan, E. Taarning, *Science* **2010**, 328, 602-605.
[13] A. Corma, L. T. Nemeth, M. Renz, S. Valencia, *Nature* **2001**, 412, 423-425.
[14] X. Tang, H. Chen, L. Hu, W. Hao, Y. Sun, X. Zeng, L. Lin, S. Liu, *Appl. Catal., B* **2014**, 147, 827-834.
[15] V. M. T. M. Silva, A. E. Rodrigues, *AIChE Journal* **2005**, 51, 2752-2768.
[16] a) M. a. R. Capeletti, L. Balzano, G. de la Puente, M. Laborde, U. Sedran, *Appl. Catal., A* **2000**, 198, L1-L4; b) V. M.T.M. Silva, A. r. E. Rodrigues, *Chem. Eng. Sci.* **2001**, 56, 1255-1263.
[17] X. He, H. Liu, *Catal. Today* **2014**, 233, 133-139.
[18] P. Li, G. Liu, H. Wu, Y. Liu, J. Jiang, P. Wu, *J. Phys. Chem. C* **2011**, 115, 3663-3670.
[19] a) J. Dijkmans, M. Dusselier, D. Gabriëls, K. Houthoofd, P. C. M. M. Magusin, S. Huang, Y. Pontikes, M. Trekels, A. Vantomme, L. Giebeler, S. Oswald, B. F. Sels, *ACS Catal.* **2015**, 5, 928-940; b) J. Dijkmans, M. Dusselier, W. Janssens, M. Trekels, A. Vantomme, E. Breynaert, C. Kirschhock, B. F. Sels, *ACS Catal.* **2016**, 6, 31-46.
[20] a) C. Hammond, S. Conrad, I. Hermans, *Angew. Chem. Int. Ed.* **2012**, 51, 11736-11739; b) P. Wolf, C. Hammond, S. Conrad, I. Hermans, *Dalton Trans.* **2014**, 43, 4514-4519.
[21] a) C. Hammond, D. Padovan, A. Al-Nayili, P. P. Wells, E. K. Gibson, N. Dimitratos, *ChemCatChem* **2015**, 7, 3322-3331; b) P. Wolf, M. Valla, F. Núñez-Zarur, A. Comas-Vives, A. J. Rossini, C. Firth, H. Kallas, A. Lesage, L. Emsley, C. Copéret, I. Hermans, *ACS Catal.* **2016**, 4047-4063.
[22] J. D. Lewis, S. Van de Vyver, A. J. Crisci, W. R. Gunther, V. K. Michaelis, R. G. Griffin, Y. Roman-Leshkov, *ChemSusChem* **2014**, 7, 2255-2265.
[23] S. Van de Vyver, C. Odermatt, K. Romero, T. Prasomsri, Y. Román-Leshkov, *ACS Catal.* **2015**, 5, 972-977.
[24] C. Wang, Y. Zhou, M. Ge, X. Xu, Z. Zhang, J. Z. Jiang, *J. Am. Chem. Soc.* **2010**, 132, 46-47.
[25] J. Dijkmans, D. Gabriëls, M. Dusselier, F. de Clippel, P. Vanelderen, K. Houthoofd, A. Malfliet, Y. Pontikes, B. F. Sels, *Green Chem.* **2013**, 15, 2777-2785.
[26] a) M. A. Camblor, A. Corma, S. Valencia, *J. Mater. Chem.* **1998**, 8, 2137-2145; b) M. M. Antunes, S. Lima, P. Neves, A. L. Magalhães, E. Fazio, A. Fernandes, F. Neri, C. M. Silva, S. M. Rocha, M. F. Ribeiro, M. Pillinger, A. Urakawa, A. A. Valente, *J. Catal.* **2015**, 329, 522-537.
[27] P. Fejes, J. B. Nagy, K. Kovács, G. Vankó, *Appl. Catal., A* **1996**, 145, 155-184.
[28] a) S. Roy, K. Bakhmutsky, E. Mahmoud, R. F. Lobo, R. J. Gorte, *ACS Catal.* **2013**, 3, 573-580; b) C. Paris, M. Moliner, A. Corma, *Green Chem.* **2013**, 15, 2101-2109; c) B. Tang, W. Dai, G. Wu, N. Guan, L. Li, M. Hunger, *ACS Catal.* **2014**, 4, 2801-2810.
[29] R. Bermejo-Deval, R. Gounder, M. E. Davis, *ACS Catal.* **2012**, 2, 2705-2713.
[30] a) A. Corma, *Chem. Rev.* **1995**, 95, 559-614; b) T. Barzetti, E. Selli, D. Moscotti, L. Forni, *J. Chem. Soc. Faraday Trans,* **1996**, 92, 1401-1407.
[31] a) R. Buzzoni, S. Bordiga, G. Ricchiardi, C. Lamberti, A. Zecchina, G. Bellussi, *Langmuir.* **1996**, 12, 930-940; b) C. Pazé, S. Bordiga, C. Lamberti, M. Salvalaggio, A. Zecchina, G. Bellussi, *J. Phys. Chem. B* **1997**, 101, 4740-4751; c) F. Bonino, A. Damin, S. Bordiga, C. Lamberti, A. Zecchina, *Langmuir.* **2003** 19, 2155-2161.
[32] C. Ngamcharussrivichai, P. Wu, T. Tatsumi, *J. Catal.* **2005**, 235, 139-149.
[33] S. Tolborg, I. Sadaba, C. M. Osmundsen, P. Fristrup, M. S. Holm, E. Taarning, *ChemSusChem* **2015**, 8, 613-617.
[34] L. Li, T. I. Korányi, B. F. Sels, P. P. Pescarmona, *Green Chem.* **2012**, 14, 1611-1619.
[35] J. P. Marques, I. Gener, P. Ayrault, J. M. Lopes, F. R. Ribeiro, M. Guisnet, *Chem Commun* **2004**, 2290-2291.
[36] A. Corma, *J. Catal.* **2003**, 215, 294-304.
[37] J. Jae, E. Mahmoud, R. F. Lobo, D. G. Vlachos, *ChemCatChem* **2014**, 6, 508-513.
[38] R. Bermejo-Deval, M. Orazov, R. Gounder, S. Hwang, M. E. Davis, *ACS Catal.* **2014**, 4, 2288-2297.
[39] M. Dusselier, P. Van Wouwe, F. de Clippel, J. Dijkmans, D. W. Gammon, B. F. Sels, *ChemCatChem* **2013**, 5, 569-575.
[40] V. L. Sushkevich, I. I. Ivanova, S. Tolborg, E. Taarning, *J. Catal.* **2014**, 316, 121-129.
[41] a) K. Tanaka, G. C. Fu, *J. Org. Chem.* **2001**, 66, 8177-8186; b) D. H. Leung, R. G. Bergman, K. N. Raymond, *J. Am. Chem. Soc.* **2007**, 129, 2746-2747.
[42] M. Dusselier, P. Van Wouwe, S. De Smet, R. De Clercq, L. Verbelen, P. Van Puyvelde, F. E. Du Prez, B. F. Sels, *ACS Catal.* **2013**, 3, 1786-1800.

Entry for the Table of Contents

FULL PAPER

The Sn-β, pre-calcined in Ar and treated with sodium-exchange exhibits the highest selectivity toward the desired MPV products.

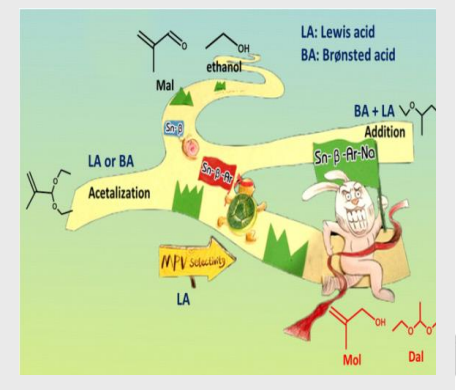

Wenda Hu, Yan Wan, Lili Zhu, Xiaojie Cheng , Shaolong Wan, Jingdong Lin and Yong Wang*

Page No. – Page No.

A Strategy for Simultaneous Synthesis of Methally Alcohol and Diethyl Acetal with Sn-β